

Photodissociation and theoretical studies of the $\text{Au}^+-(\text{C}_5\text{H}_5\text{N})$ complex

Hsu-Chen Hsu,^a Fang-Wei Lin,^a Chun-Chia Lai,^b Po-Hua Su^a and Chen-Sheng Yeh^{*a}

^a Department of Chemistry, National Cheng Kung University, Tainan, Taiwan 701, R.O.C.
E-mail: csyeh@mail.ncku.edu.tw

^b Department of Chemistry, National Changhua University of Education, Changhua, Taiwan 50058, R.O.C.

Received (in Montpellier, France) 8th October 2001, Accepted 20th November 2001

First published as an Advance Article on the web

Laser vaporization combined with a supersonic molecular beam was employed to generate and study the $\text{Au}(\text{C}_5\text{H}_5\text{N})^+$ complex for the first time. On the basis of the ionization energies (IE) between gold and pyridine, the $\text{Au}(\text{C}_5\text{H}_5\text{N})^+$ species is viewed as being a $\text{Au}^+-\text{C}_5\text{H}_5\text{N}$ species. Photodissociative charge transfer was observed with exclusive $\text{C}_5\text{H}_5\text{N}^+$ (pyridine) formation. The photofragmentation spectrum of $\text{Au}^+-(\text{C}_5\text{H}_5\text{N})$ was scanned by monitoring the pyridine fragments. A structureless continuum spectrum was observed and the onset of $\text{C}_5\text{H}_5\text{N}^+$ appearance indicates the upper limit on the $\text{Au}^+-\text{C}_5\text{H}_5\text{N}$ bond strength to be $59.6 \text{ kcal mol}^{-1}$. *Ab initio* calculations at the MP2 level were employed to optimize the geometries of the gold complexes and binding energies were obtained using CCSD(T) single point calculations. Besides from the C_{2v} structure observed in Cu^+ and Ag^+ complexes, the theoretical results yielded a second isomer with C_1 symmetry which is 24 kcal mol^{-1} less stable in energy than the C_{2v} isomer.

Metal ion–molecule complexes are especially of interest in the areas of catalysis, organometallic chemistry and biological sciences. There is no doubt that the bond energy is of central importance for understanding the thermodynamic aspects of metal–molecule interactions. The electrostatic or covalent nature of the bonding has been described for a variety of complexes.^{1–3} In our continued efforts to investigate the chemical and physical processes involving metal cations and heterocyclic molecules in the gas phase, we have now studied the isolated $\text{Au}(\text{C}_5\text{H}_5\text{N})^+$ complex.

In metal ion–molecule complexes, the third-row transition metals have received much less attention as compared to the large amount of data available for first- and second-row transition metals, in both experimental and theoretical studies. The heavy Au^+ is of particular interest because of the pronounced relativistic effects that it may exhibit.⁴ These result in electron transfer from ligands to Au^+ and increases the covalent binding between Au^+ and the ligands. In this respect, Schwarz and co-workers have studied the complexation of Au^+ with a series of ligands, such as F, CO, H_2O , NH_3 , C_2H_4 , C_3H_6 , C_6H_6 and C_6F_6 , quite extensively.^{2,5} Experimental and theoretical results revealed that the binding of Au^+ to several ligands is distinctly different from the other transition metals. In particular, an exceptionally large relativistic stabilization was observed in both Au^+-NH_3 and $\text{Au}^+-\text{C}_2\text{H}_4$ complexes.⁵ Using the radiative association kinetics method, Dunbar and co-workers investigated the reactions of Au^+ and Au^- with C_6H_6 and C_6F_6 as well.⁶

The photodissociation technique has proven to be an effective way to probe bond strengths of ion species.⁷ Recently, we obtained an upper limit for the binding energies of the $\text{M}^+-\text{pyridine}$ complexes ($\text{M}^+ = \text{Cu}^+, \text{Ag}^+$) with C_{2v} structures by observing a photodissociative charge transfer (CT) fragment (the pyridine cation).^{8,9} In this report, the $\text{Au}(\text{C}_5\text{H}_5\text{N})^+$ complex was generated for the first time and laser excitation was employed to inspect its photochemical behavior and ground-state binding energy. The structures and binding energies of the Au complexes

were also obtained from *ab initio* calculations, which showed there were two isomers with C_{2v} and C_1 symmetries.

Experimental

The details of the experimental setup were described previously.⁹ The $\text{Au}(\text{C}_5\text{H}_5\text{N})^+$ complex was generated using laser vaporization combined with a supersonic molecular beam source. A gold foil (99.9%) was wrapped around an Al rod and the target rod was suspended in a cutaway holder, which is a rod holder without a growth channel to produce primarily ion complexes containing one and/or two ligands. The rotating and translating rod was irradiated using the 532 nm wavelength of the second harmonic output from a Nd:YAG laser operated at 10 Hz with $1\text{--}2 \text{ mJ pulse}^{-1}$. The vaporization laser beam was focused 1.5 cm in front of the metal rod. Prior to seeding the pyridine vapor, pure He gas (6 atm) was used to inspect the ion products from our source. It was found that only the Au^+ atomic signal appeared, and that no other impurities, such as Al^+ and metal oxides, were detected. Ion complexes containing pyridine expanded adiabatically and were skimmed into a reflectron time-of-flight mass spectrometer, followed by mass selection of $\text{Au}(\text{C}_5\text{H}_5\text{N})^+$ for carrying out the photodissociation experiments. An unfocused dissociation laser (pulsed tunable dye laser pumped by an Nd:YAG laser) crossed the ion beam at the turning point in the reflector. The wavelength-dependent spectrum was measured by recording the intensity of the fragment as a function of the dissociation laser wavelength. The laser fluence was kept low ($\sim 1.2 \text{ mJ cm}^{-2}$) to minimize multiphoton absorption. The fragment power dependence revealed a linear relation with fluence up to at least 7 mJ cm^{-2} .

Theoretical computations

The calculations were performed using second-order Møller–Plesset perturbation theory (MP2). The double-zeta valence

basis sets and the effective core potentials (ECPs) of Hay and Wadt were used for the Au atom¹⁰ and the 6-31G(d,p) set was selected for C, H, and O. The relativistic effects were included in the Hay–Wadt ECPs of Au. We also added f polarization functions to increase the flexibility of the ECP basis set. The f exponent was 1.050 for Au.¹¹ The MP2/6-31G(d,p) level was employed to fully optimize the geometries of the ligand, transition state and ion complexes and the resulting harmonic vibrational frequencies were used to evaluate the zero-point energy corrections. CCSD(T) single point calculations with the corresponding MP2/6-31G(d,p) zero-point energies were derived from CCSD(T)/6-31G(d,p)//MP2/6-31G(d,p) calculations. All calculations were performed using the Gaussian 98 suite of programs.¹²

Results and discussion

Fig. 1(a) shows both the Au^+ and $\text{Au}(\text{C}_5\text{H}_5\text{N})^+$ mass peaks, where the experimental conditions were adjusted to generate ion species in the low mass range. From the viewpoint of their ionization energies (IE), the positive charge should be localized on the Au atom, which has an IE of 9.22 eV, lower than that of the pyridine molecule (IE = 9.26 eV).^{13,14} The associated pyridine adduct is viewed as being Au^+ –pyridine. However, the IE difference between Au and pyridine is only 0.92 kcal mol^{−1} (0.04 eV). It is possible that the charge transfer reaction of Au^+ with pyridine gives rise to $\text{C}_5\text{H}_5\text{N}^+$, followed by formation of the Au^+ – $\text{C}_5\text{H}_5\text{N}^+$ condensation product in the ion source. In this case the $\text{C}_5\text{H}_5\text{N}^+$ peak should have a high probability of being observed in addition to Au^+ and $\text{Au}(\text{C}_5\text{H}_5\text{N})^+$ in the mass spectrum, if the pyridine cation is formed in the beam

source. We saw no ions other than the product channels assigned in Fig. 1(a), that is no $\text{C}_5\text{H}_5\text{N}^+$. It is worthy of mention that in our studies on the $\text{Au}(\text{furan})^+$ system, where furan has a lower IE (8.89 eV) than that of the Au atom, we readily observed the molecule cation signal, furan^+ .¹⁵ Although it is most likely that the positive charge resides on the Au atom, Au –pyridine⁺ complex formation cannot be excluded completely. It is interesting to note that Dunbar and co-workers used the radiative association methodology to study the reaction of Au^+ with C_6H_6 .⁶ Benzene has a similar IE (9.25 eV) to that of pyridine.¹⁴ Their results indicated that the Au^+ charge transfer reaction accompanied by C_6H_6^+ formation has a rate constant close to zero. Such an experimental approach will be valuable to understand the possibility of charge transfer between Au^+ and pyridine.

Photodissociation was performed on the mass-selected $\text{Au}(\text{C}_5\text{H}_5\text{N})^+$ complex, as shown in Fig. 1(b). The resulting fragment ion appeared as $\text{C}_5\text{H}_5\text{N}^+$. Since the Au^+ – $\text{C}_5\text{H}_5\text{N}$ complex is the parent signal, the photodissociation induces a ligand-to-metal CT. The same experimental results were obtained when the laser excited pyridine complexes containing Cu^+ and Ag^+ .^{8,9} The photofragment spectrum over the 435–485 nm wavelength region is given in Fig. 2. Throughout the experiments, the parent ion intensity remained approximately constant. Due to the limitation of our dye laser, the spectrum could not be recorded in the 366–430 nm region. The pyridine daughter ion was the only fragment observed during the photodissociation process. No $\text{C}_5\text{H}_5\text{N}^+$ channel could be detected between 472.7 and 485 nm, as seen in Fig. 2. The threshold of photofragment appearance was determined to be 472.3 nm, at which wavelength the $\text{C}_5\text{H}_5\text{N}^+$ was barely seen, and the pyridine intensity continuously increased as the excitation wavelength was scanned towards the blue. As mentioned above, a photo-induced dissociative CT has taken place from the Au^+ – $\text{C}_5\text{H}_5\text{N}$ complex. On the basis of the energetic diagram shown in Fig. 3, the lowest CT state correlating to $\text{Au}^+(\text{S}) + \text{C}_5\text{H}_5\text{N}^+$ is only 0.92 kcal mol^{−1} (0.04 eV) above the $\text{Au}^+(\text{S}) + \text{C}_5\text{H}_5\text{N}(\text{A}_1)$ states corresponding to the Au^+ – $\text{C}_5\text{H}_5\text{N}$ ground state. Excitation of Au^+ – $\text{C}_5\text{H}_5\text{N}$ into the dissociation limit of the lowest CT electronic state is a direct step yielding $\text{C}_5\text{H}_5\text{N}^+$ product, whereas dissociative CT may also involve a transition to a higher electronic surface, followed by electronic curve crossing to the $\text{Au}^+(\text{S}) + \text{C}_5\text{H}_5\text{N}^+$ asymptote. It should be noted that the interpretation of the dissociative mechanism has been restricted to a one-photon absorption. A two-photon excitation cannot be ruled out if the absorption cross-section is significantly different for the two steps, while the power dependence measurement exhibits a linear relation.

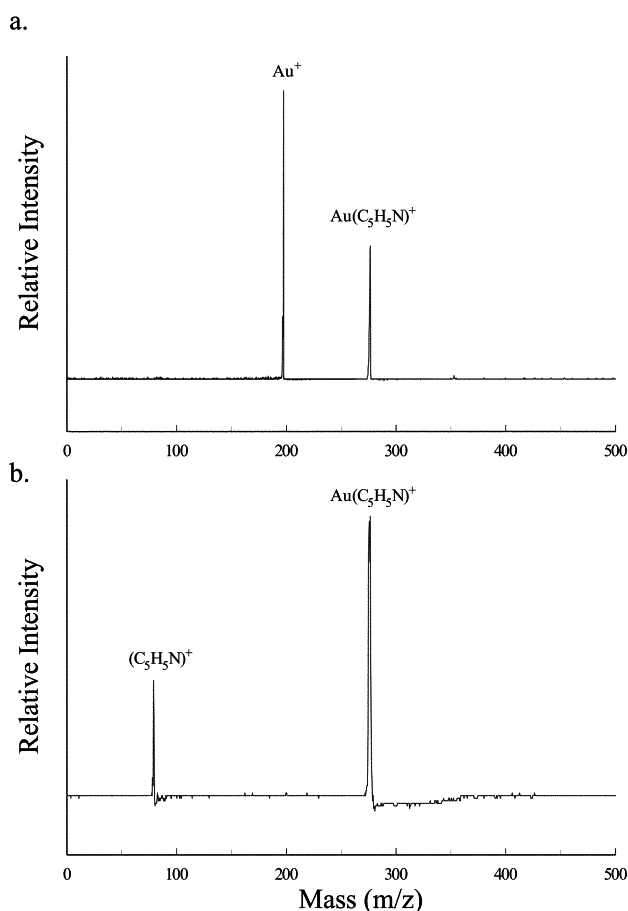


Fig. 1 (a) Mass spectrum of Au^+ and $\text{Au}(\text{C}_5\text{H}_5\text{N})^+$. (b) Photofragmentation mass spectrum of mass-selected $\text{Au}(\text{C}_5\text{H}_5\text{N})^+$ at 355 nm with 5 mJ cm^{−2} light fluence.

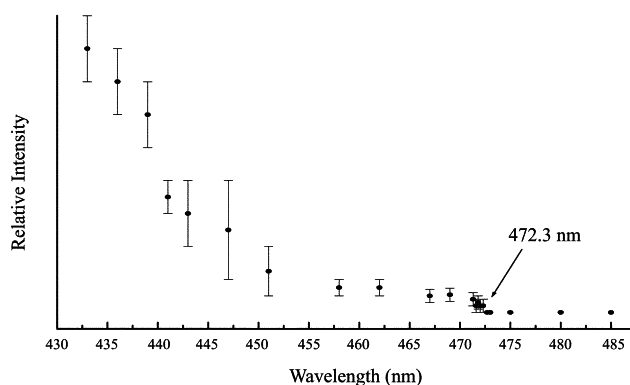


Fig. 2 Photofragmentation spectrum of $\text{Au}(\text{C}_5\text{H}_5\text{N})^+$ obtained by monitoring the pyridine cation signal as a function of laser wavelength. The arrow indicates the threshold of pyridine appearance. The error bars represent the fragment intensity deviations. Each data point is an average of two or three measurements.

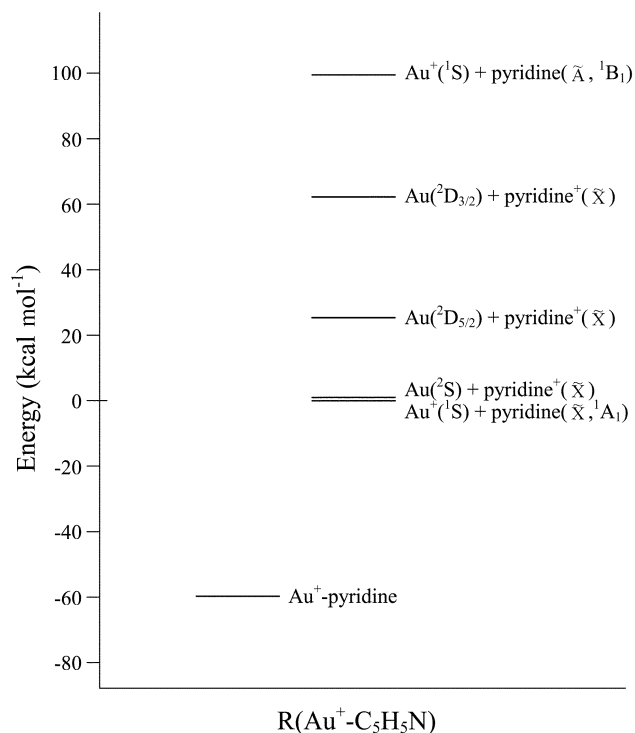


Fig. 3 Energy level diagram displaying the asymptotic states corresponding to gold and pyridine. The Au^+ -pyridine ground state lies $59.6 \text{ kcal mol}^{-1}$ below the $\text{Au}^+(^1\text{S}) + \text{pyridine}(^1\text{A}_1)$ reference level, as determined from the photodissociation experiments.

Taking the CT threshold (472.3 nm) as a reference, the upper bound of the binding energy (BDE) in the ground state can be derived from the following relation:

$$h\nu \geq D_0'' + \Delta\text{IE}$$

ΔIE represents the IE difference ($0.92 \text{ kcal mol}^{-1}$) between Au and pyridine. The upper limit on the $\text{Au}^+-\text{C}_5\text{H}_5\text{N}$ bond strength was calculated to be $59.6 \text{ kcal mol}^{-1}$. As reported previously, the same experimental method was employed to study pyridine complexes containing Cu^+ and Ag^+ .^{8,9} The observed upper limit BDEs are 65.5 and $45.2 \text{ kcal mol}^{-1}$ for $\text{Cu}^+-\text{C}_5\text{H}_5\text{N}$ and $\text{Ag}^+-\text{C}_5\text{H}_5\text{N}$, respectively. $\text{Au}^+-\text{C}_5\text{H}_5\text{N}$ has a slightly smaller BDE than $\text{Cu}^+-\text{C}_5\text{H}_5\text{N}$ and a greater one than $\text{Ag}^+-\text{C}_5\text{H}_5\text{N}$. For the complexation of Au^+ with other nitrogen base ligands, ion-molecule reactions using the bracket methodology performed by Schwarz and co-workers led to a binding energy of $71 \pm 7 \text{ kcal mol}^{-1}$ for the Au^+-NH_3 complex.^{3c}

Theoretical approaches as well were employed to obtain the complex geometry and binding energies. MP2/6-31G(d,p) was used to fully optimize the complex structures. Earlier studies showed that the optimizations of the pyridine complexes containing Cu and Ag ended up with the C_{2v} minimum.^{8,9} The metal atoms lie off the the nitrogen atom and effect a slight distortion on the pyridine structure. The Au complex was revealed to also have C_{2v} symmetry (Fig. 4) with BDEs of 69.9 and $67.0 \text{ kcal mol}^{-1}$ in the MP2 and CCSD(T) calculations, respectively. The complexation of Au^+ with a series of ligands investigated by Schwarz and co-workers indicated that partial electron transfer occurred from the ligands to the gold metal ion, resulting in increased covalent interactions between Au^+ and the ligands due to the relativistic effects in the gold atom.^{2,5} Considering the π orbital electrons of the pyridine as possible candidates to undergo electron transfer, one isomeric structure with C_1 symmetry was observed in which the Au atom resided over the C_1-C_2 bond and was slightly shifted outside the perimeter of the ring, as depicted in Fig. 4(a). Such

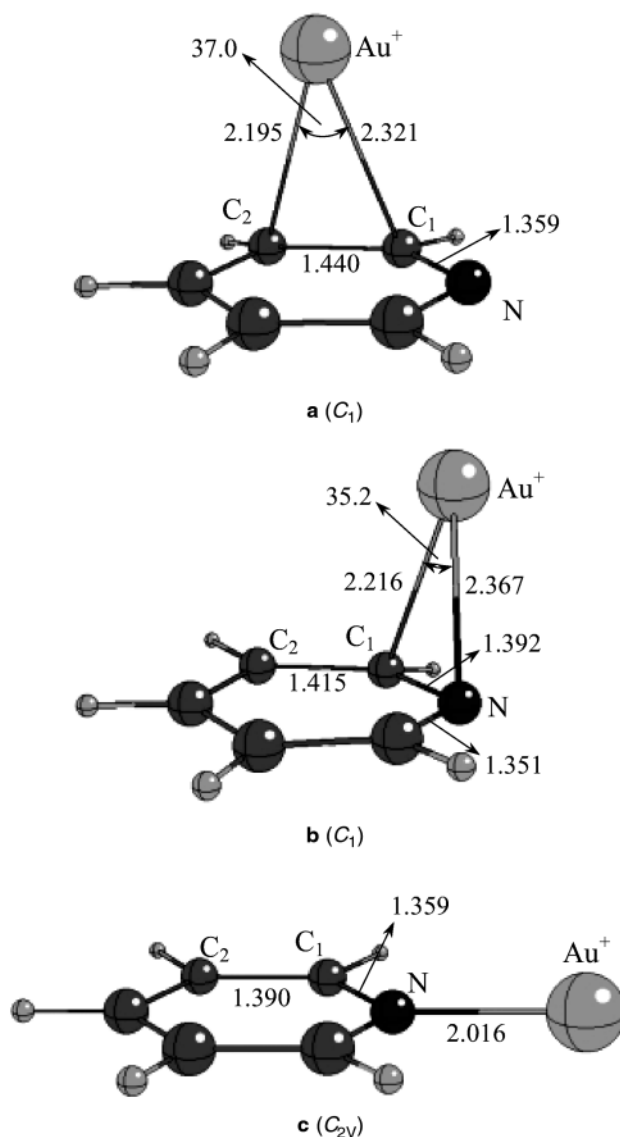


Fig. 4 Geometrical parameters of the stationary points of the $[\text{Au}^+, \text{C}_5\text{H}_5\text{N}]$ potential energy surface. The parameters were calculated at the MP2/6-31G(d, p) level of theory. Selected lengths in angstroms and bond angles in degrees.

a binding site in C_1 geometry could also be seen in the interaction of Au^+ with the benzene molecule, studied by Koch and co-workers.¹⁶ This intermediate state is bound by $43.0 \text{ kcal mol}^{-1}$ [CCSD(T)] relative to the separated Au^+ and $\text{C}_5\text{H}_5\text{N}$. Such a stable intermediate was not found in the pyridine complexes containing Cu^+ and Ag^+ .^{8,9} As shown in Fig. 5, **a** and **c** are connected by a transition structure **b**, which has Au^+ lying over the C_1-N bond, and the activation barrier was estimated to be $5.8 \text{ kcal mol}^{-1}$ for the $\text{C}_1 \rightarrow \text{C}_{2v}$ isomerization. Although a stable intermediate state **a** was observed, it remains to clarify whether or not the relativistic effects in Au play a key role for such an observation. A detailed theoretical analysis is required to resolve this question.

Table 1 lists the binding energies of the M^+ -pyridine complexes ($\text{M}^+ = \text{Cu}^+, \text{Ag}^+, \text{and Au}^+$). The calculated binding energies from either MP2 or CCSD(T) show that the gold complex with a C_{2v} structure has the strongest binding as compared to the copper and silver complexes. As mentioned earlier and from the results shown for the Cu^+ and Ag^+ complexes, the employed photodissociation technique resulting in CT would provide an upper limit for the binding energy in the ground state. Our determined upper binding energy is

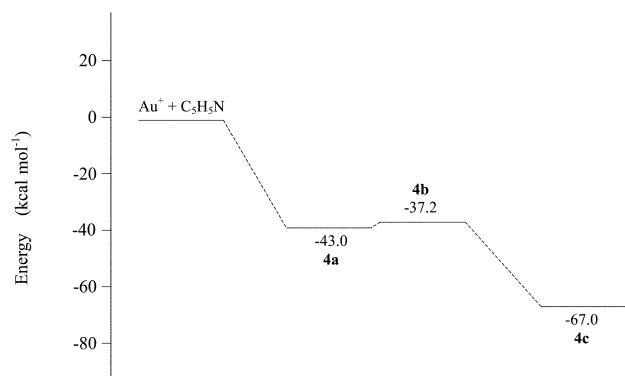


Fig. 5 Potential energy surface for the interaction of Au^+ with $\text{C}_5\text{H}_5\text{N}$. The energies were obtained with the CCSD(T)/6-31G(d,p)//MP2/6-31G(d,p) method.

Table 1 Binding energies (D_0 in kcal mol^{-1}) for metal–pyridine complexes

Complex	Symmetry	Method	D_0
Cu^+ -pyridine ^a	C_{2v}	MP2/6-31G(d, p)	57.8
		Exptal.	65.6
Ag^+ -pyridine ^a	C_{2v}	MP2/6-31G(d, p)	39.3
		Exptal.	45.2
Au^+ -pyridine	C_{2v}	MP2/6-31G(d, p)	69.9
	C_{2v}	CCSD(T)/6-31G(d, p)//MP2/6-31G(d, p)	67.0
	C_1	MP2/6-31G(d, p)	47.5
	C_1	CCSD(T)/6-31G(d, p)//MP2/6-31G(d, p)	43.0
		Exptal.	59.7

^a Taken from ref. 8.

located between the **a** and **c** complex values. It is possible that the **a** isomer was synthesized in our cluster source. However, **c** formation cannot be ruled out, since two possible factors, internally hot ions and a two-photon excitation mechanism, need to be considered as possibly leading to an artificially low experimental threshold. Using Ar as the carrier gas provides a way to cool vibrationally excited ions. The results indicated that the onset of pyridine appearance remained constant regardless of the gas properties. Another possible contribution is that two-photon absorption might take place at the photodissociation threshold. Dunbar and Honovich showed that one-photon behavior could occur if a small fraction of one-photon ions together with two-photon species were present in the threshold region.¹⁷ The photofragment kinetic energy is the other uncertainty in the course of complex dissociation, with consideration of the kinetic shift resulting in the true onset appearing shifted towards the red. In a survey of previous studies using the same experimental strategy as employed here, photodissociation performed on the Ag^+ –benzene complex by Duncan *et al.* resulted in an upper binding energy of 30 kcal mol^{-1} ,¹⁸ $6.5 \text{ kcal mol}^{-1}$ less than the theoretical prediction.¹⁹ It also should be mentioned that further theoretical calculations using better basis sets should give a more confident binding energy for the Au ion complex. At this stage, our experiments cannot justify the prepared Au^+ – $\text{C}_5\text{H}_5\text{N}$ identity

from the cluster source. On the basis of the theoretical prediction at the CCSD(T) level of theory, the CT dissociation threshold of the C_{2v} isomer is determined to lie at 421 nm. It would be helpful to conduct the photodissociation signal search in the 366–430 nm region, which is inaccessible to our dye laser.

Acknowledgement

We thank the National Science Council of the Republic of China for its financial support for this work.

References

- 1 C. W. Bauschlicher and H. Partridge, *J. Phys. Chem.*, 1991, **95**, 3946.
- 2 J. Hrušák, D. Schröder and H. Schwarz, *Chem. Phys. Lett.*, 1994, **225**, 416.
- 3 C. N. Yang and S. J. Klippenstein, *J. Phys. Chem. A*, 1999, **103**, 1094.
- 4 P. Pykkö, *Chem. Rev.*, 1988, **88**, 563.
- 5 See, for example: (a) P. Schwerdtfeger, J. S. McFeaters, M. J. Liddell, J. Hrušák and H. Schwarz, *J. Chem. Phys.*, 1995, **103**, 245; (b) J. Hrušák, R. H. Hertwig, D. Schröder, P. Schwerdtfeger, W. Koch and H. Schwarz, *Organometallics*, 1995, **14**, 1284; (c) D. Schröder, H. Schwarz, J. Hrušák and P. Pykkö, *Inorg. Chem.*, 1998, **37**, 624; (d) R. H. Hertwig, W. Koch, D. Schröder, H. Schwarz, J. Hrušák and P. Schwerdtfeger, *J. Phys. Chem.*, 1996, **100**, 12253.
- 6 Y.-P. Ho and R. C. Dunbar, *Int. J. Mass Spectrom. Ion Processes*, 1999, **182/183**, 175.
- 7 S. W. Buckner and B. S. Freiser, *Polyhedron*, 1988, **7**, 1583.
- 8 Y. S. Yang, W. Y. Hsu, H. F. Lee, Y. C. Huang, C. S. Yeh and C. H. Hu, *J. Phys. Chem. A*, 1999, **103**, 11287.
- 9 Y. S. Yang and C. S. Yeh, *Chem. Phys. Lett.*, 1999, **305**, 395.
- 10 P. J. Hay and W. R. Wadt, *J. Chem. Phys.*, 1985, **82**, 299.
- 11 A. W. Ehlers, M. Böhme, S. Dapprich, A. Gobbi, A. Höllwarth, V. Jonas, K. F. Köhler, R. Stegmann, A. Veldkamp and G. Frenking, *Chem. Phys. Lett.*, 1993, **208**, 111.
- 12 M. J. Frisch, G. W. Trucks, H. B. Schlegel, G. E. Scuseria, M. A. Robb, J. R. Cheeseman, V. G. Zakrzewski, J. A. Montgomery, Jr., R. E. Stratmann, J. C. Burant, S. Dapprich, J. M. Millam, A. D. Daniels, K. N. Kudin, M. C. Strain, O. Farkas, J. Tomasi, V. Barone, M. Cossi, R. Cammi, B. Mennucci, C. Pomelli, C. Adamo, S. Clifford, J. Ochterski, G. A. Petersson, P. Y. Ayala, Q. Cui, K. Morokuma, D. K. Malick, A. D. Rabuck, K. Raghavachari, J. B. Foresman, J. Cioslowski, J. V. Ortiz, A. G. Baboul, B. B. Stefanov, G. Liu, A. Liashenko, P. Piskorz, I. Komaromi, R. Gomperts, R. L. Martin, D. J. Fox, T. Keith, M. A. Al-Laham, C. Y. Peng, A. Nanayakkara, C. Gonzalez, M. Challacombe, P. M. W. Gill, B. Johnson, W. Chen, M. W. Wong, J. L. Andres, C. Gonzalez, M. Head-Gordon, E. S. Replogle, J. A. Pople, *Gaussian 98*, rev. A.7, Gaussian, Inc., Pittsburgh, PA, 1998.
- 13 E. Moore, *Atomic Energy Levels*, National Bureau of Standards, Washington DC, 1971.
- 14 G. Herzberg, *Electronic Spectra and Electronic Structure of Polyatomic Molecules*, Van Nostrand Reinhold, New York, 1966.
- 15 P. H. Su, F. W. Lin and C. S. Yeh, *J. Phys. Chem. A*, 2001, **105**, 9643.
- 16 T. K. Dargel, R. H. Hertwig and W. Koch, *Mol. Phys.*, 1999, **96**, 583.
- 17 R. C. Dunbar and J. P. Honovich, *Int. J. Mass Spectrom. Ion Processes*, 1984, **58**, 25.
- 18 K. F. Willey, P. Y. Cheng, M. B. Bishop and M. A. Duncan, *J. Am. Chem. Soc.*, 1991, **113**, 4721.
- 19 C. W. Bauschlicher, H. Partridge and S. R. Langhoff, *J. Phys. Chem.*, 1992, **96**, 3273.